

THE POTENTIAL FOR GOLD MINERALISATION IN THE GREENSTONE BELT OF BUSIA DISTRICT, SOUTH EASTERN UGANDA

¹A. B. Mbonimpa, ²E. Barifaijo and ³J. V. Tiberindwa
Email: ebarifaijo@sci.mak.ac.ug; alexmbonimpa@yahoo.com

¹P.O. Box 25095-00603, Nairobi

^{2,3}Department of Geology, Makerere University. P. O. Box 7062, Kampala, Uganda

ABSTRACT:- Busia district in south eastern Uganda is one of the areas in the country with a history of potential for gold mineralisation and exploitation. Gold was first discovered in the Archaean greenstone belt of Busia by Davies in 1932. Only small mining operations, mostly artisan in character, have taken place in the district since then except the newly opened mines by Busitema Mining Company. However, all recent work in the area indicates potential for gold exploitation. Both quartz vein-hosted and Banded Iron Formation (BIF)-hosted gold deposits occur in Busia district. The results of Electron Microprobe (EMP) analysis of 10 rock samples from the quartz vein deposits and AAS analysis of 10 rock, 27 soil and 18 stream sediment samples taken from Busia district are presented in this work. Gold occurs as electrum or native gold inclusions in pyrite with fineness in the range of 451 – 863; and as invisible gold in sulphide minerals (up to 5700 ppm in pyrite). The main ore minerals are pyrite, magnetite, ilmenite, galena, pyrrhotite, chalcopyrite, covellite and rutile. Gold values of the stream sediment samples average 7.7 ppm Au, the highest being 38.6 ppm Au. Soil sampling was done in the three areas proposed for follow-up by Mroz et al. (1991), of which the Tira area has the first priority soil anomaly (up to 4.8 ppm Au) followed by the Osapiri area (up to 2.8 ppm Au). There is a strong correlation between the distribution of lead and that of gold.

Key words: Busia district, Archaean greenstone belt, quartz vein-hosted gold deposits, banded iron formation-hosted deposits, sulphides.

INTRODUCTION

The Busia gold deposits are in the Archaean greenstone belt of south eastern Uganda which extends into south western Kenya and north eastern Tanzania and forms part of the Tanzanian craton. The location of the present study is in the sub-counties of Buteba and Busitema and is bounded to the north by River Malaba; to the west and south by River Solo and to the east by the Kenyan border; and by longitudes 34° 00' E and 34° 08' E; and latitudes 0° 28' N and 0° 35' N (Fig. 1). There are two main types of primary deposits; the auriferous quartz veins that are preferentially located in the basic metavolcanic facies and the Banded Iron Formations (BIF) where gold may be disseminated and/or occur in sulphide-bearing quartz veinlets (Mroz et al., 1991). Gold was first discovered in Busia by Davies of the Geological Survey and Mines Department (GSMD) in 1932. This was initially followed by a rush by various prospectors but preliminary results concerning grade and volume were not encouraging and

by 1935 only the GSMD was still doing exploration work in the area. It is estimated that the cumulative production between 1937 and 1944, when the major workings ceased, was 443 kg Au and that between 1949 and 1961, small mining operations, more artisan in character, yielded between 1.0 and 1.5 t Au (Mroz et al., 1991). Artisan gold mining has been going on since then in Busia and other parts of Uganda and today gold is the third leading export of Uganda. There has been renewed interest in the Busia area by the GSMD and by some private firms (e.g. Bureau de recherches géologiques et minières (BRGM) and Roraima Mining Co. Ltd.) and some of their studies have indicated potential for gold exploitation in the Busia area. Busitema Mining Co. Ltd. has recently opened a mine at the old workings in the Tira sector and remains the only operational mine in Busia area. Further north, in the Amonikakinei sector, according to Mroz et al. (1991), exploration work by GSMD in 1938-39 led to the discovery of two gold-rich reefs: the Baurle's reef (300 m, 11.6 g/ton) and the Geophysical reef (600m, between 0.7 and 59 g/ton). These old workings remain abandoned.

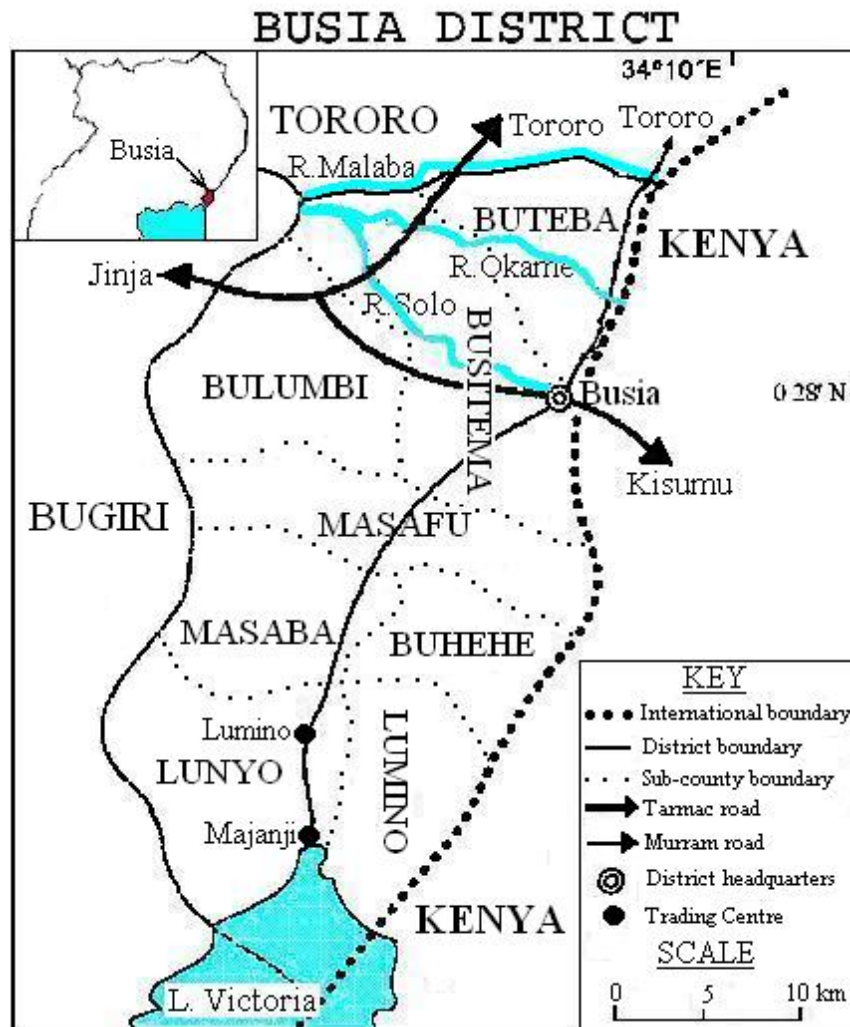


Figure 1: Map of Busia district showing Study Area. Inset: Map of Uganda showing location of Busia district (Adapted from Rwabwoogo, 1998)

In the BRGM report, Mroz et al. (1991) recommended follow-up work in three areas of Tira, Osapiri and Bukade-Makina (Fig. 2). In the present work, a soil survey using a grid of 250 x 1000 m was done in these areas and anomalies of 4.8 ppm Au in Tira and 2.8 ppm Au in Osapiri were found. Stream sediment sampling was also done and values of up to 38.6 ppm Au were noted. Some rock

samples were taken from the underground mine operated by Busia Mining Co. Ltd. Electron Microprobe (EMP) analysis of these rocks was also done and gold was found to occur as native gold or electrum inclusions in pyrite and as invisible gold in sulphide minerals, the most important being pyrite.

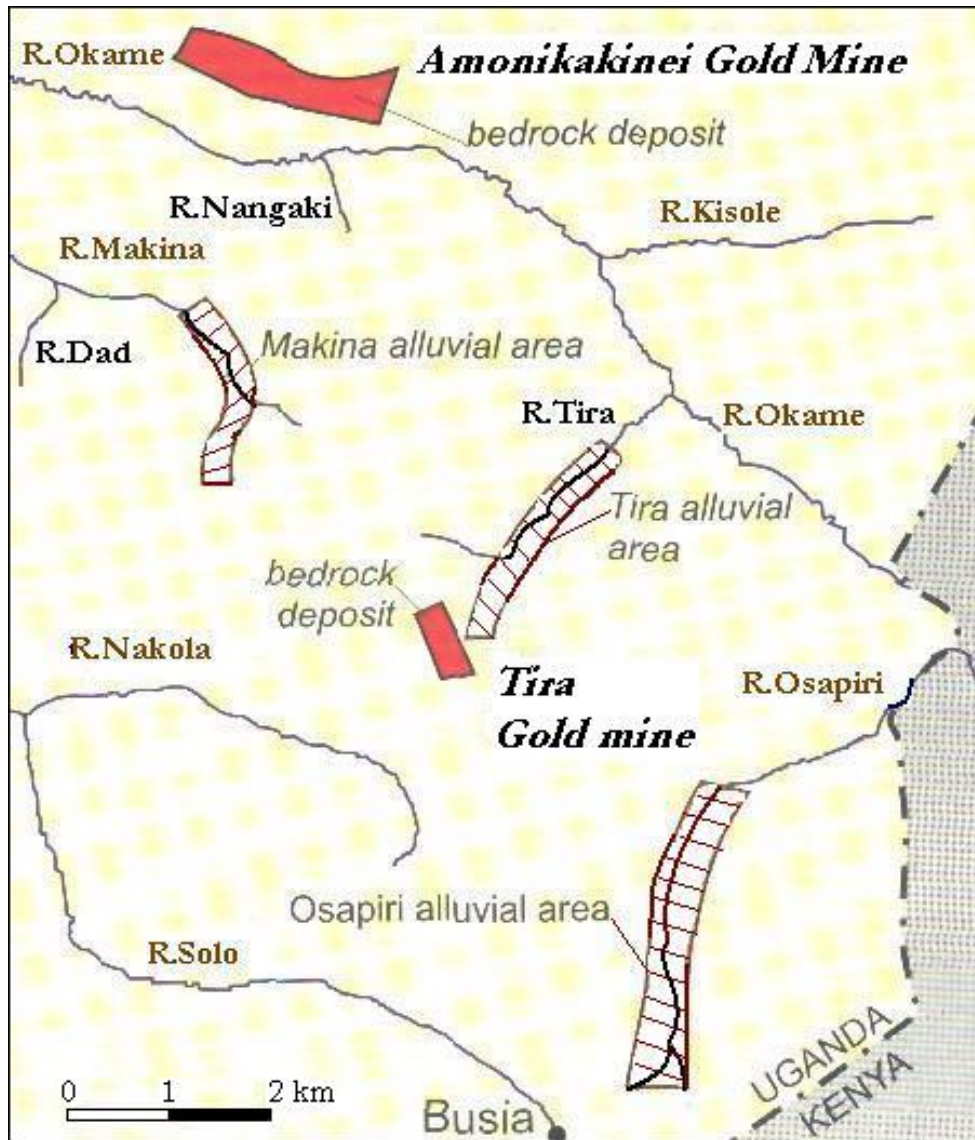


Figure 2: Mineralised areas in Busia district including the three areas (shaded) recommended for follow-up by Mroz et al. (1991) (From Hester & Boberg, 1996)

GEOLOGICAL SETTING

The geology of the area consists of Nyanzian-Kavirondian volcano-sedimentary formations (Fig. 3) belonging to the Archaean greenstone belt that extends into south western Kenya and north eastern Tanzania (Old, 1968). These rocks form the northern part of the Tanzanian

craton. The rock types include banded quartzites, ironstones, phyllites, greywackes, conglomerates and acid to basic lavas and tuffs. The metavolcanic and metasediment series are separated by a ferruginous banded quartzite that forms an important marker horizon. The formations are intruded by granite bodies (e.g. Masaba and Buteba) of Archaean age (Old, 1968) and have undergone greenschist facies metamorphism.

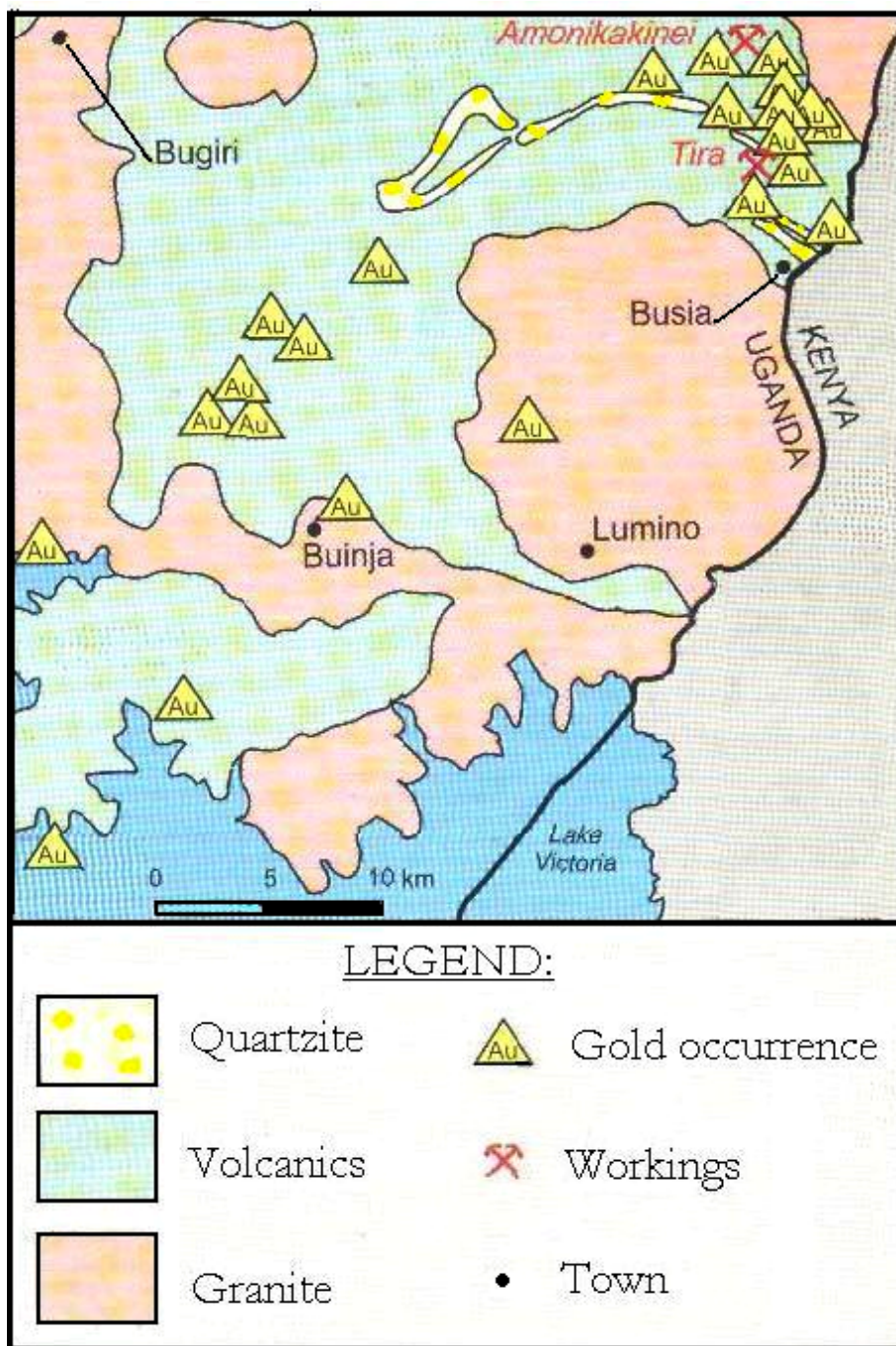


Figure 3: Geological map of Busia area showing gold occurrences (Adapted from Hester & Boberg, 1996)

SAMPLES AND METHODOLOGY

The present study involved taking 66 rock, 40 stream sediment and 82 soil samples and making field observations and measurements (e.g. structures). 26 of the rock samples were picked from the underground mine at Tira and from these, 10 samples rich in visible sulphides were selected to make 21 polished sections at the Institute of Mineralogy and Petrology, Hamburg University (IMPHU). The remaining pieces of these samples were ground to fine powder which was analysed for different elements by AAS (Table 4).

The polished sections were studied systematically by a reflected light microscope in order to identify gold/electrum/silver inclusions. EMP analysis of these inclusions and other ore minerals was done at IMPHU using a CAMECA SX – 100 wavelength dispersive instrument in the standard programme mode. The analytical conditions were: an accelerating voltage of 20.0 kV for the electrum inclusions and sulphide minerals and 15.0 kV for oxide minerals; a beam current of 20 nA and a beam diameter of about 1 μm . The standards used in the analyses for the different elements were pure metals for Ag, Au, Bi, Co, Fe and Ni; chalcopyrite for Cu, vanadinite for Pb and andradite for Si, Ca and Fe; and synthetic minerals FeAsS for As; FeS₂ for S; SbS₃ for Sb; MnTiO₃ for Mn and Ti; ZnS for Zn; Al₂O₃ for Al; MgO for Mg and Cr₂O₃ for Cr. The X-ray lines used were K α for S, Pb, Fe, Cu, Mn, Co, Ni, Zn, Al, Si, Mg, Ti, Ca and Cr; L α for As, Ag, Sb and Au; and M α for Pb and Bi.

In addition, 22 soil samples from the areas recommended for follow up by Mroz et al. (1991); 5 samples taken vertically from an open pit at the Tira mine and 18 stream sediment samples taken from streams in the study area at an interval of about 0.5 km (Table 5); were analysed by a PERKIN-ELMER 2380 AAS machine for Au, Ag, Cu, Ni, Zn, Pb and MnO. The samples were dried overnight in an oven at 105 °C, ground to fine size with a porcelain mortar and pestle, sieved and digested. The portion less than 63 μm was used to analyse for gold while that less than 125 μm but greater than 63 μm was used to analyse for the other elements. The very fine portion was used for gold in order to reduce the nugget effect on sample representativity and analytical reproducibility. One way of reducing the effect would be to collect larger samples than the conventional 5-20 g. This is technically sound but often impractical (Closs, 1997). On the other hand, by using an “ultra-fine” gold (< 5 μm) fraction and a sensitive

method for gold (detection limit 0.2 ppb), conventional samples of 5 to 20 g are sufficient to provide reproducible regional anomalies for subsequent follow-up (Xie and Wang, 1991). In the present study, as a means of striking a balance between these two approaches, a particle size of less than 63 μm and samples of about 500 g (from which a representative sample was got by the coning and quartering method) were used. After digestion, Methyl Isobutyl Ketone (MIBK) was used to extract the gold from the acid solution.

RESULTS

Ore Minerals

The rock samples selected for EMP analysis were those rich in visible sulphides and this was not the case with the BIF hosted deposits in which mineralisation is probably disseminated. The results of the EMP analysis are therefore of the quartz vein hosted deposits. These were formed by mineralising fluids that intruded the country rock through already existing NW-trending fractures. The fluids also altered the country rock leading to the formation of secondary minerals like chlorite, sericite, epidote, zoisite, calcite, sphene and goethite.

The major ore minerals are pyrite, magnetite and ilmenite. Others include electrum, galena, chalcopyrite, covellite, pyrrhotite and rutile. Pyrite is the most abundant ore mineral and occurs mostly as subhedral to euhedral grains of all sizes up to about 2mm. It hosts other ore minerals as inclusions. Electrum occurs as inclusions in pyrite (Fig. 4) of <20 μm (but usually about 5 μm) and is intergrown with pyrrhotite or galena inclusions in some pyrite grains (Fig. 5). Chalcopyrite and pyrrhotite occur preferentially as subhedral inclusions of <50 μm in pyrite while magnetite, ilmenite, rutile and galena mostly form as independent minerals. Galena grains in the silicate matrix are usually subhedral and about 150 μm . Magnetite occurs mostly as euhedral elongated grains of <50 μm while ilmenite mostly occurs as polymorphs with a colloform texture and size of about 100 μm . Covellite mostly forms rims around pyrite grains (Fig. 6) but sometimes occurs as elongate grains of about 25 μm . Intergrowths of different minerals are common especially of magnetite-pyrite-chalcopyrite (Fig. 7), pyrrhotite-galena-electrum (Fig. 5) or pyrrhotite-chalcopyrite. Pyrite in many samples has undergone alteration such that it appears as if it is intergrown with sphalerite. However, EMP analysis and element mapping (Fig. 8) show that it is goethite (resulting from alteration) and not sphalerite.

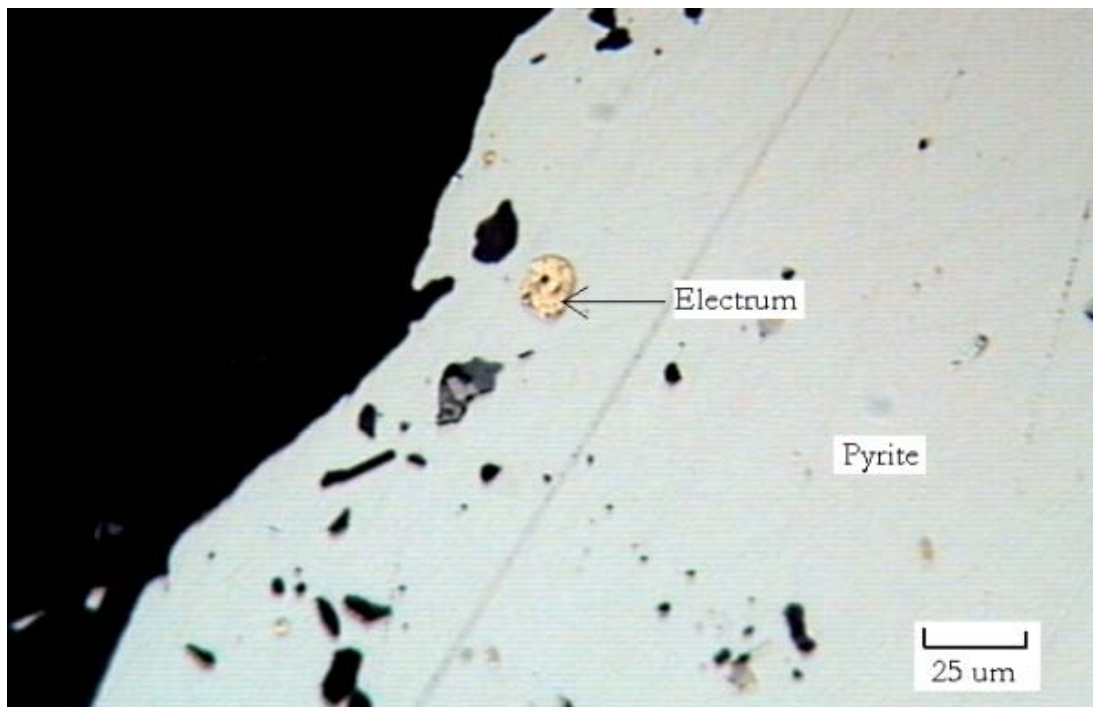


Figure 4: Photomicrograph of Sample AM40-3-1 showing an electrum grain in pyrite

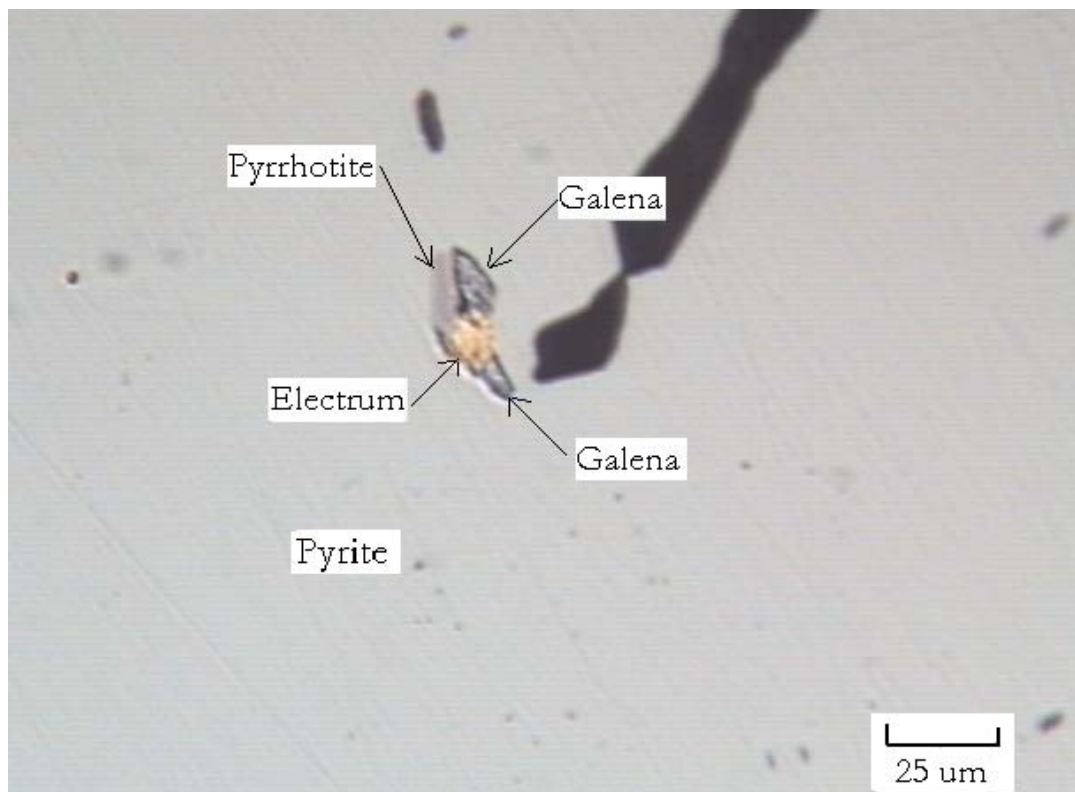


Figure 5: Photomicrograph of Sample AM16-2-1 showing electrum inter-grown with other minerals

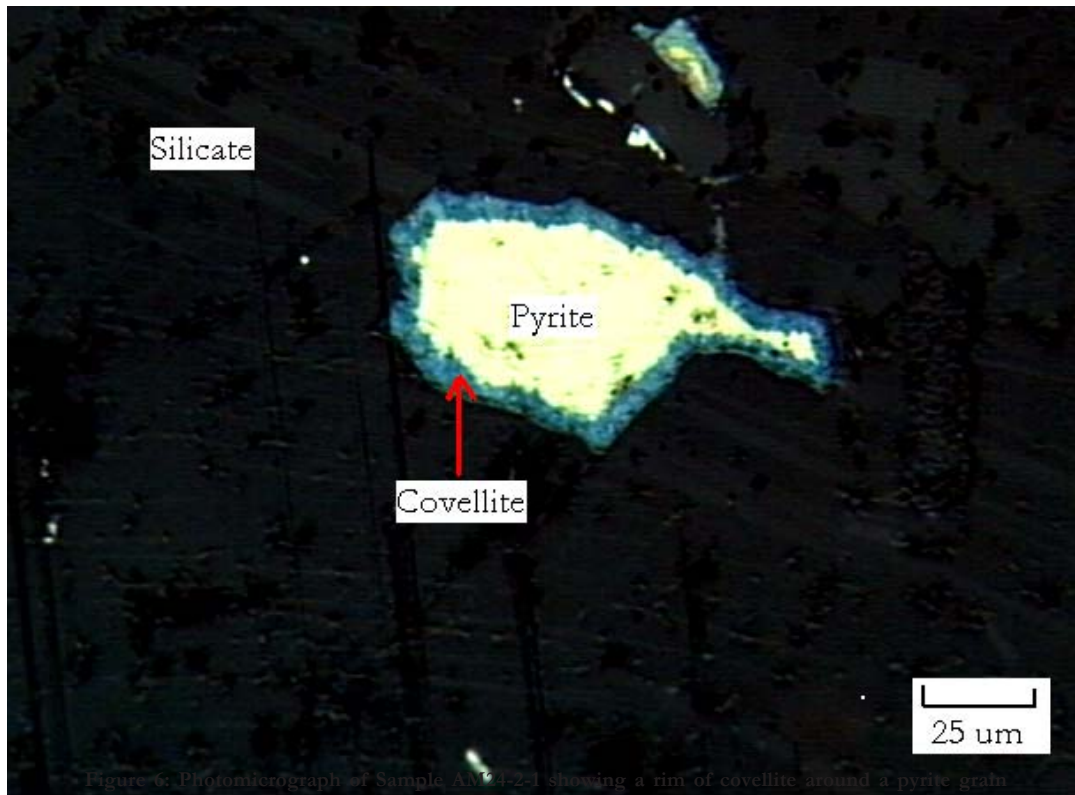


Figure 6: Photomicrograph of Sample AM24-2-1 showing a rim of covellite around a pyrite grain

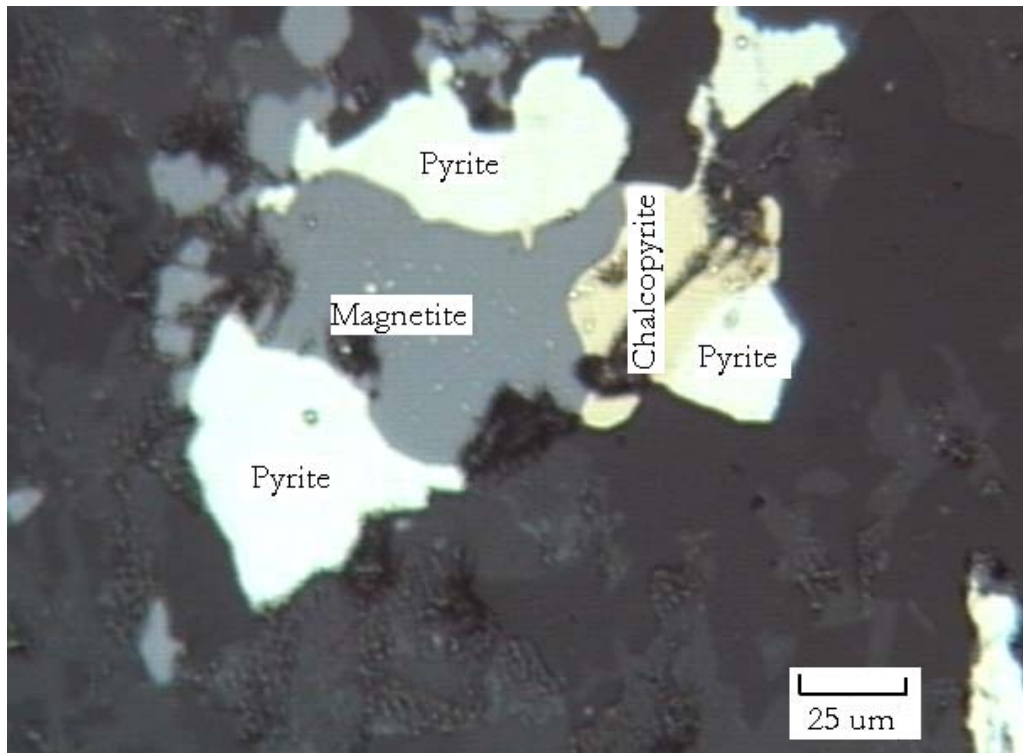


Figure 7: Photomicrograph of Sample AM17-2-1 showing mineral intergrowths

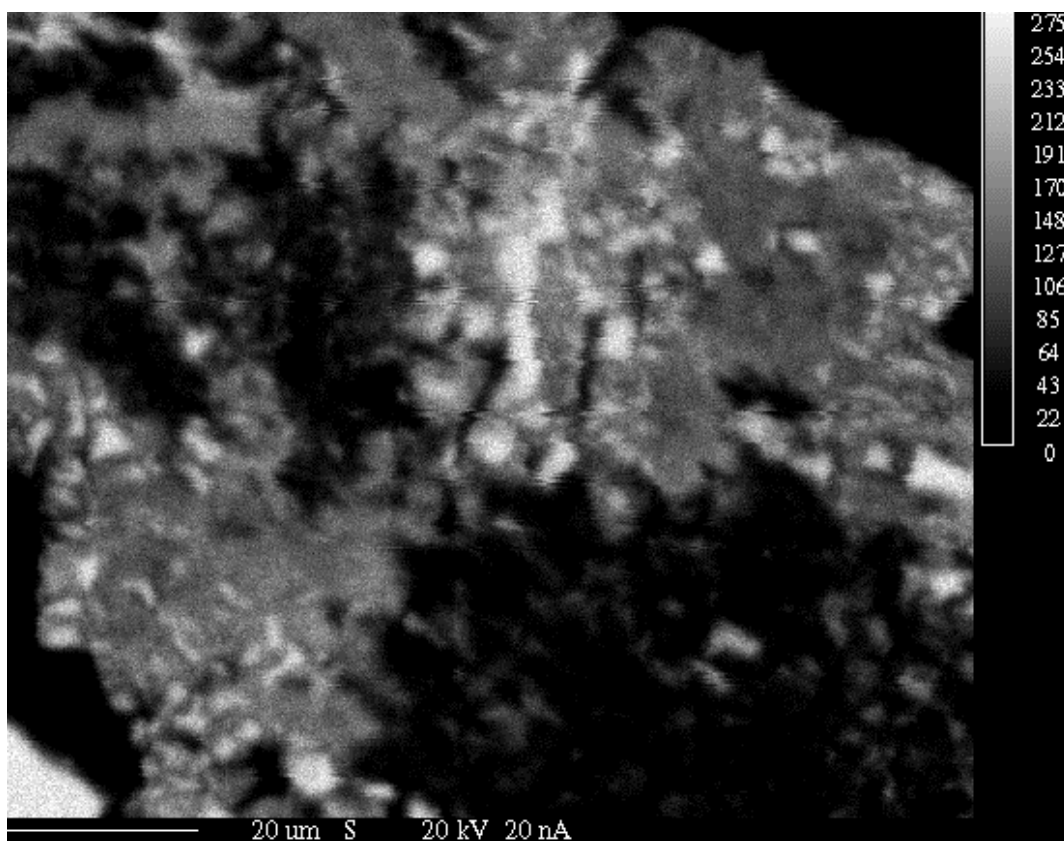


Figure 8: A S-element map of Sample AM33-2-5a. The dark parts (along diagonal from top left to right bottom corner) have been altered to goethite

Gold Mineralisation

In Rock Samples

Gold in the Busia quartz vein deposits occurs as electrum or native gold inclusions in pyrite or as invisible gold in the sulphide minerals. The inclusions are solid solutions of gold with silver together with trace amounts of Bi, Pb and Cu (Table 1). Fineness ranges from 451 – 863. Element mapping and Back Scattered Electron (BSE) photomicrographs of some grains show that Au, Ag and Bi are distributed homogeneously in the grains (Figs. 9 – 12).

Analyses of pyrite, chalcopyrite, pyrrhotite and galena show that, gold not only occurs as inclusions in pyrite but also as invisible gold in these minerals (Table 2). 35 analyses of these minerals were done and 19 of these indicate presence of gold. Pyrrhotite analyses are in the range of 0 – 0.47 wt% Au (5 analyses, only one of which

was 0%) while galena is between 0 – 0.52 wt% Au (14 analyses). The galena that occurs as inclusions in pyrite has gold while that in the silicate matrix mostly has no gold. Chalcopyrite analyses range from 0 – 0.04 wt% Au (9 analyses) while those of pyrite are between 0 – 0.57 wt% Au (7 analyses). Given that pyrite is much more abundant than other sulphide minerals, it is the most important host of invisible gold. Several grains of magnetite and ilmenite were analysed for different elements (Table 3) and no gold was found in any of them. Ilmenite has high manganese contents while magnetite has low manganese and titanium contents.

Silver values are between 0 – 0.68 wt% for all the minerals, with the highest values in galena. Arsenic values are between 0 – 0.11 wt%. It tends to substitute for sulphur in all sulphides except galena. However the extent of its substitution is minimal and therefore not important as a control of gold distribution. Unlike in the electrum/gold grains, there is no bismuth in the ore minerals.

In addition to EMP analysis, the samples were also analysed for whole rock metal content by AAS (Table 4). The highest value obtained was 6.8 ppm Au. Lead has a very high correlation of +0.9 with gold.

In Soil and Stream Sediment Samples

45 samples were analysed by AAS for Au, Ag, Cu, Ni, Zn, Pb and MnO (Table 6). There are a number of stream sediments from Tira, Aget and Nakola rivers with high concentrations of gold, 38.6 ppm Au being the highest value. Samples from the soil grids are generally <2ppm Au. There is an anomaly of 4.8 ppm Au about half a kilometre north of the present Tira mine and another of 2.8 ppm Au in the Osapiri area. The Osapiri area has a number

of samples with >1ppm Au but the values in the Bukade-Makina area are generally <1ppm Au. The Tira area has the most significant gold anomalies of the areas recommended for follow-up by Mroz et al. (1991).

The anomalies of gold (Fig. 13) coincide with those of Pb (Fig. 14), Cu (Fig. 15), Ag and Zn but are completely different from those of Ni (Fig. 16). Like gold, the above elements (except Ni) have three anomalies at UTM coordinates (619000, 55000), (620000, 56500) and (619500, 58000).

The soil samples taken from the open pit at Tira mine are in the range of 0.8 – 7.4 ppm Au with the concentration generally increasing upwards (Table 5).

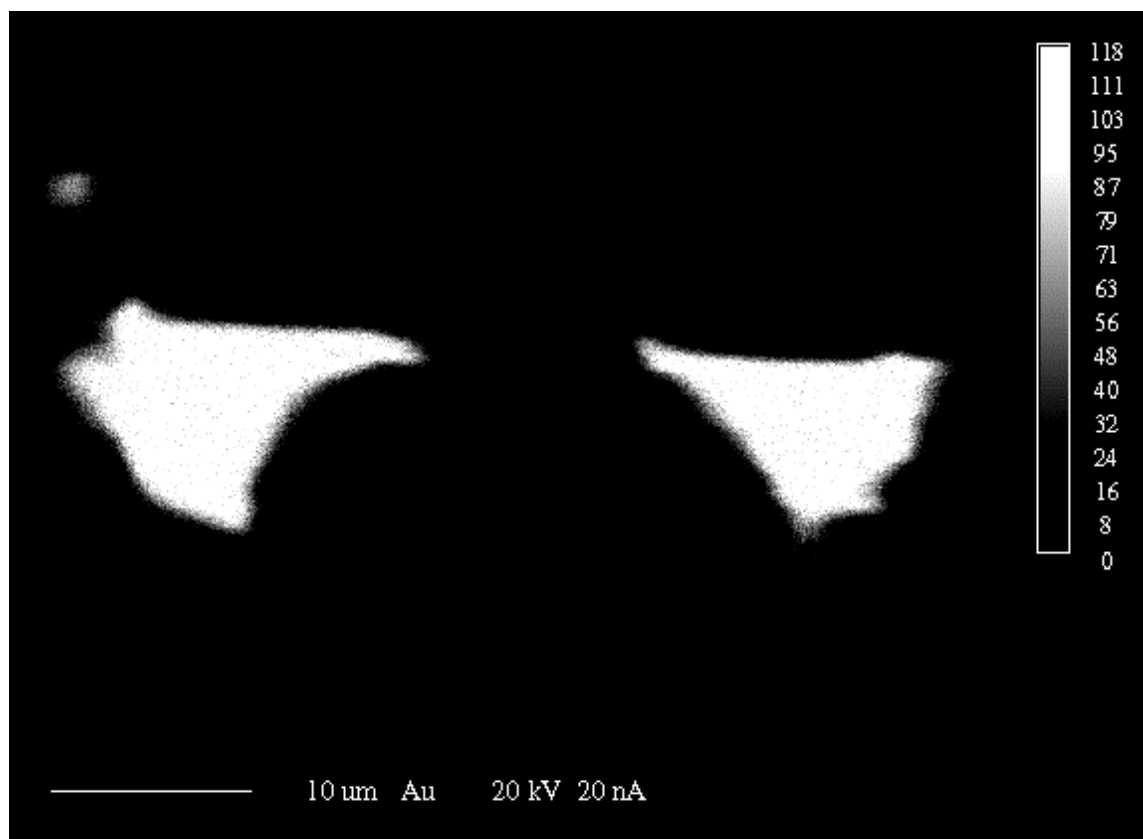


Figure 9: An Au-element map of two electrum grains showing its homogeneous distribution

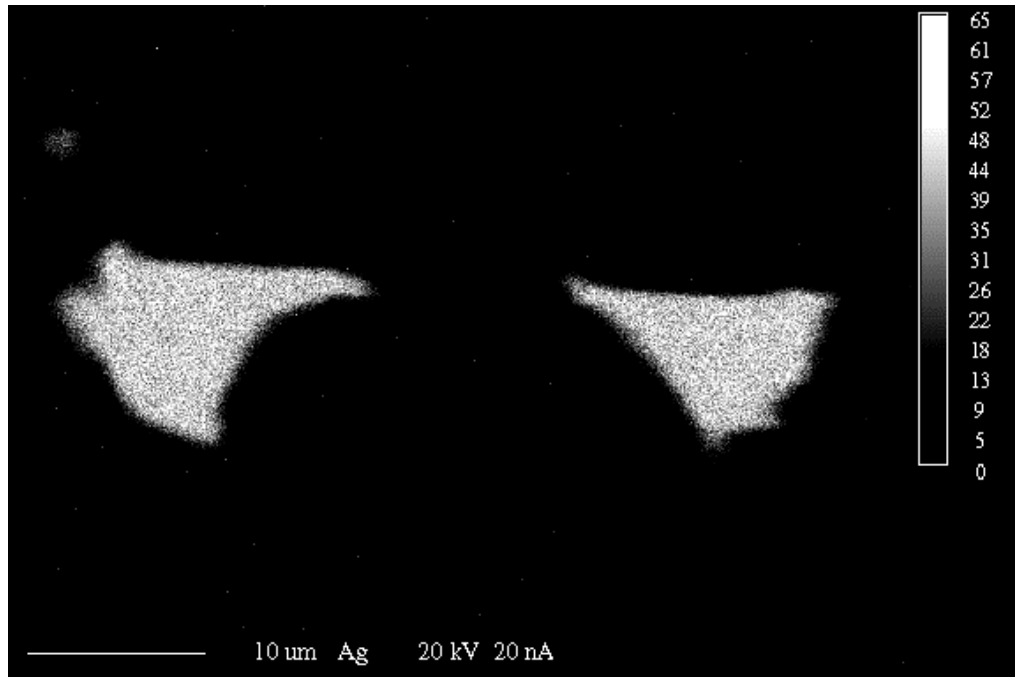


Figure 10: A Ag-element map of the same electrum grains showing its homogeneous distribution

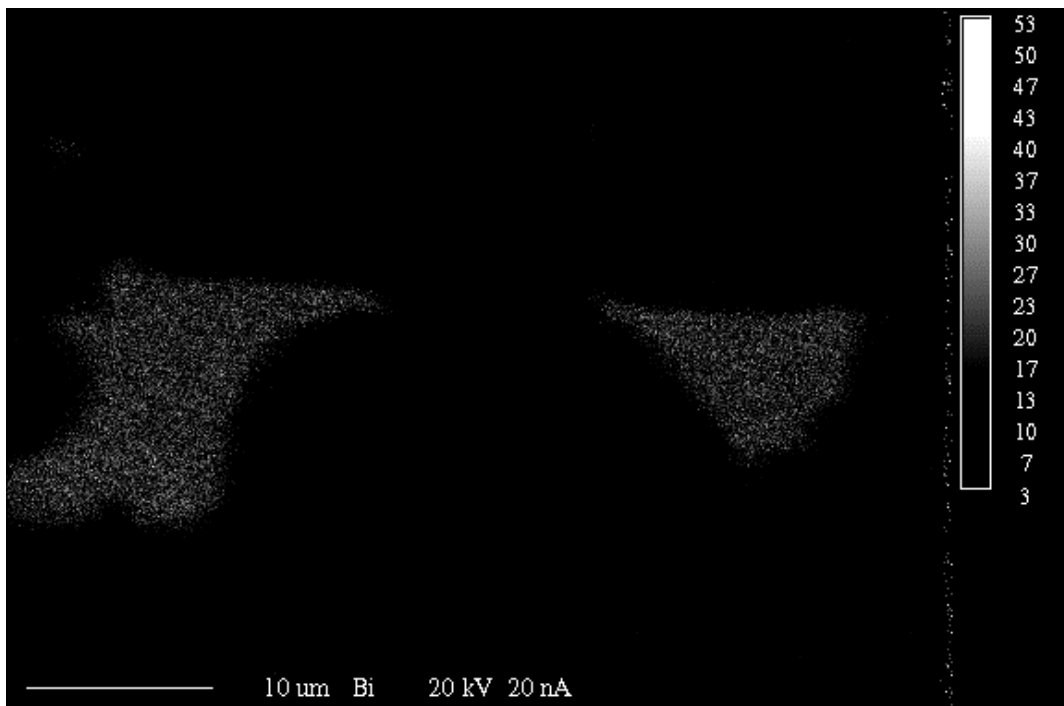


Figure 11: A Bi-element map of the same electrum grains showing its homogeneous distribution

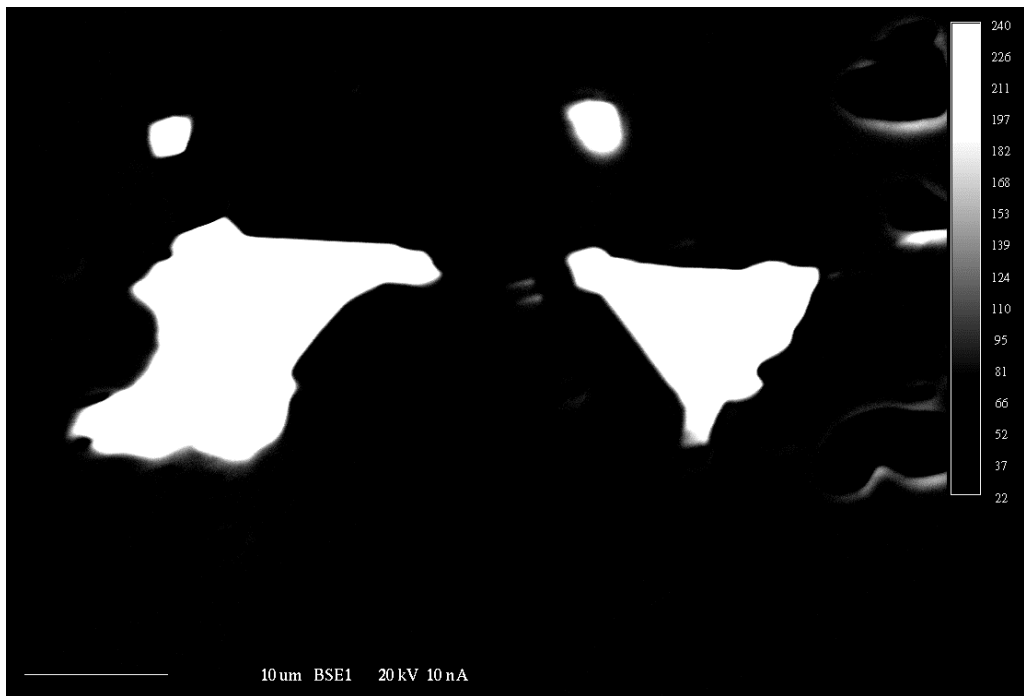


Figure 12: A BSE map of the same electrum grains showing the homogeneous distribution of the high atomic number (Au, Ag and Bi) elements

Table 1: Results of electron microprobe analysis of ‘electrum’ grains in weight %

	SAMPLE	Au	Ag	Cu	Bi	Pb	Total	Stoichiometry	Fineness
#1	AM16-2-1a	88.45	8.56	0.03	0.31	0.08	97.35	Au _{0.85} Ag _{0.15}	850
#2	AM16-2-1b	88.36	8.27	0.01	0.33	0	96.97	Au _{0.85} Ag _{0.15}	854
#3	AM23-1-1a	58.68	39.16	0.03	0.14	-	98	Au _{0.45} Ag _{0.55}	451
#4	AM38-1-1a	75.65	21.1	0.2	0.37	0	97.33	Au _{0.66} Ag _{0.33}	663
#5	AM40-1-2a	61.61	36.11	0.06	0.29	-	98.07	Au _{0.48} Ag _{0.52}	483
#6	AM40-1-2c	62.71	34.66	0.03	0.23	-	97.63	Au _{0.50} Ag _{0.50}	498
#7	AM40-2-1a	70.58	29.67	0	0.04	-	100.29	Au _{0.57} Ag _{0.43}	566
#8	AM40-2-1b	69.22	29.92	0	0.06	-	99.19	Au _{0.56} Ag _{0.44}	559
#9	AM40-2-3a	69.54	31.81	0	0.28	0.1	101.63	Au _{0.54} Ag _{0.45}	545
#10	AM40-2-3b	67.24	34.02	0	0.38	0.06	101.64	Au _{0.51} Ag _{0.47}	520
#11	AM40-2-3c	71.03	32.43	0.05	0.35	0.37	103.86	Au _{0.52} Ag _{0.47}	525
#12	AM40-3-1a	88.63	9.56	0.04	0.26	0.89	98.48	Au _{0.83} Ag _{0.16}	835
#13	AM40-3-1b	86.77	7.52	7.52	7.52	-	94.58	Au _{0.86} Ag _{0.14}	863
#14	AM40-3-1c	87.99	7.68	0	0.25	-	95.92	Au _{0.86} Ag _{0.14}	862
#15	AM40-3-2a	85.01	13.33	0.01	0.35	0.34	98.7	Au _{0.77} Ag _{0.22}	777
#16	AM40-3-2b	67.6	29.08	0	0.41	0	97.09	Au _{0.56} Ag _{0.44}	560

Table 2: Results of electron microprobe analysis of different sulphide mineral grains in weight %

	SAMPLE	Fe	S	As	Cu	Mn	Pb	Co	Ni	Zn	Ag	Sb	Bi	Au	Total	Stoichiometry	Mineral
#1	AM16-2-1b	58.65	40.1	0.05	0	0.04	0	0	0	0	0	0	0	0.24	99.08	Fe _{5.93} S _{7.06}	pyrrhotite
#2	AM16-2-1c	1.41	13.47	0	0	0.03	86.75	0	0	0.04	0	0	0	0.19	101.9	(Pb _{0.97} Fe _{0.06})S _{0.97}	galena
#3	AM16-2-1d	1.71	13.32	0	0.01	0.02	87.01	0	0	0	0.02	0	0	0.4	102.51	(Pb _{0.97} Fe _{0.07})S _{0.96}	galena
#4	AM16-2-1e	45.97	53.59	0.11	0	0.01	0	0	0	0.05	0.12	0	0	0.11	99.97	Fe _{0.99} S _{2.00}	pyrite
#5	AM33-1-1a	47.01	51.99	0.07	0.09	0	0	0	0	0	0.01	0	0	0	99.192	Fe _{1.02} S _{1.97}	pyrite
#6	AM33-1-1b	30.32	34.64	0.06	33.77	0	0	0	0	0.01	0.02	0	0	0	98.82	Cu _{0.99} Fe _{1.00} S _{2.00}	Chalcopyrite
#7	AM33-1-1c	60.16	38.74	0.07	0.07	0.02	0	0	0.01	0	0	0	0	0.08	99.19	Fe _{8.00} S _{8.97}	pyrrhotite
#8	AM33-1-4a	46.96	52.35	0.05	0.02	0.03	0	0	0.06	0.01	0.07	0	0	0	99.55	Fe _{1.02} S _{1.98}	pyrite
#9	AM33-1-4b	59.84	38.97	0.07	0	0.01	0	0	0.05	0.02	0.02	0	0	0.15	99.15	Fe _{7.95} S _{9.02}	pyrrhotite
#10	AM33-2-7a	31.29	34.69	0.05	32.75	0	0	0	1.53	0	0.04	0	0	0	100.35	Cu _{0.95} (Fe _{1.03} Ni _{0.05})S _{1.98}	chalcopyrite
#11	AM33-2-8a	30.86	34.94	0.06	33.8	0	0	0	0	0	0.01	0	0	0.04	99.71	Cu _{0.98} Fe _{1.02} S _{2.00}	chalcopyrite
#12	AM33-2-8b	31.09	34.49	0.1	33.28	0	0	0	0	0	0	0	0	0.04	99	Cu _{0.97} Fe _{1.03} S _{1.99}	chalcopyrite
#13	AM33-2-8c	60.67	39.31	0.05	0.06	0	0	0	0	0	0	0	0	0.47	100.56	(Fe _{7.99} Au _{0.02} (S _{9.00} As _{0.01}))	pyrrhotite
#14	AM34-1-1	30.92	34.97	0.02	32.73	0	0	0	0.01	0.01	0.01	0	0.04	0	98.71	Cu _{0.95} Fe _{1.02} S _{2.02}	chalcopyrite
#15	AM34-1-2b	31.12	35.13	0.04	33.01	0	0	0	0.03	0.01	0	0	0	0	99.34	Cu _{0.96} Fe _{1.03} S _{2.02}	chalcopyrite
#16	AM34-1-4a	29.17	34.45	0.04	34.99	0.01	0	0	0	0	0.06	0	0	0	98.72	Cu _{1.03} Fe _{0.97} S _{2.00}	chalcopyrite
#17	AM34-1-5b	31.18	34.75	0.02	33.06	0	0	0	0	0.02	0.03	0	0	0	99.05	Cu _{0.96} Fe _{1.03} S _{2.00}	chalcopyrite
#18	AM38-1-1b	2.12	12.81	0	0.31	0	86.1	0	0.02	0	0.07	0	0	0	101.44	(Pb _{0.97} Fe _{0.09} Cu _{0.01})S _{0.93}	galena
#19	AM38-1-1c	46.37	53.01	0.07	0.06	0	0	0	0.04	0	0.19	0	0	0.57	100.34	Fe _{1.02} S _{1.98}	pyrite
#20	AM38-1-1d	2.07	12.86	0	0.42	0	85.11	0	0	0.01	0	0	0	0	100.51	(Pb _{0.96} Fe _{0.09} Cu _{0.02})S _{0.94}	galena
#21	AM40-1-2b	1.04	12.83	0	0.02	0	85.84	0	0	0.05	0.11	0	0	0.23	100.12	(Pb _{0.99} Fe _{0.04})S _{0.96}	galena
#22	AM40-1-3a	0	13.05	0	0	0	83.45	0	0.03	0	0.58	0	0	0	97.11	(Pb _{0.99} Ag _{0.01})S _{1.00}	galena
#23	AM40-1-3b	0	13.03	0	0	0	82.7	0.01	0	0.01	0.68	0	0	0.06	96.51	(Pb _{0.98} Ag _{0.02})S _{1.00}	galena
#24	AM40-1-3c	0.01	13.12	0	0.04	0	85.12	0.02	0	0	0.45	0	0	0	98.76	(Pb _{1.00} Ag _{0.01})S _{0.99}	galena
#25	AM40-1-3d	0	12.82	0	0	0.01	83.36	0	0	0.02	0.63	0	0	0	96.84	(Pb _{0.99} Ag _{0.01})S _{0.99}	galena
#26	AM40-1-4a	0.77	12.88	0	0.02	0	85.18	0	0	0	0.47	0	0	0	99.31	(Pb _{0.99} Ag _{0.01})S _{0.97}	galena
#27	AM40-2-1c	1.58	13.21	0	0	0.01	85.98	0	0	0.01	0.09	0	0	0.52	101.41	(Pb _{0.97} Au _{0.01})S _{0.96}	galena
#28	AM40-2-4a	2.01	13.35	0	0	0	85.31	0	0	0	0.4	0	0	0	101.07	(Pb _{0.95} Fe _{0.08} Ag _{0.01})S _{0.96}	galena
#29	AM40-2-5b	60.9	39.4	0.08	0	0	0	0	0	0	0.04	0	0	0	100.42	Fe _{7.99} (S _{9.00} As _{0.01})	pyrrhotite
#30	AM40-2-Za	30.9	36.23	0	33.19	0	0	0	0.02	0.01	0	0	0	0.04	100.39	Cu _{0.95} Fe _{1.00} S _{2.05}	chalcopyrite
#31	AM40-2-Zb	2.01	13.18	0	0.31	0	87.03	0	0.02	0	0.19	0	0	0.07	102.82	(Pb _{0.96} Fe _{0.08} Cu _{0.01})S _{0.94}	galena
#32	AM40-3-1d	46.88	52.64	0.07	0.01	0	0	0	0.01	0.07	0	0	0	0.06	99.73	Fe _{1.01} S _{1.98}	pyrite
#33	AM40-3-2c	0.47	12.71	0	0	0.01	83.94	0	0	0	0.27	0	0	0	97.4	(Pb _{1.00} Fe _{0.02} Ag _{0.01})S _{0.98}	galena
#34	AM40-3-2d	46.7	52.48	0.08	0	0.02	0	0	0.02	0.01	0.08	0	0	0.32	99.71	Fe _{1.01} S _{1.98}	pyrite
#35	AM40-3-2e	47.02	52.96	0.02	0	0	0	0	0.02	0	0	0	0	0.22	100.23	Fe _{1.01} S _{1.99}	pyrite

Table 3: Results of electron microprobe analysis of oxide mineral grains in wt %

	SAMPLE	Si	Ti	Al	Cr	Fe	Mn	Mg	Ca	Zn	O	Total	Mineral
#1	AM16-1-1a	0.04	31.72	0.01	0.01	30.99	5.43	0.00	0.06	0.34	31.82	100.43	ilmenite
#2	AM16-1-1b	0.12	31.28	0.00	0.00	27.64	8.02	0.01	0.42	0.16	31.49	99.14	ilmenite
#3	AM16-1-1c	0.02	0.07	0.02	0.04	70.89	0.08	0.00	0.00	0.01	20.44	91.58	magnetite
#4	AM16-1-2a	0.08	31.59	0.03	0.01	27.64	8.51	0.01	0.29	0.00	31.74	99.9	ilmenite
#5	AM33-2-1a	0.01	31.94	0.00	0.00	28.17	8.71	0.01	0.04	0.07	32.00	100.96	ilmenite
#6	AM33-2-1b	0.65	0.19	0.18	0.03	69.74	0.12	0.07	0.11	0.00	21.15	92.24	magnetite
#7	AM33-2-1c	0.40	0.15	0.15	0.00	69.94	0.09	0.06	0.04	0.00	20.81	91.63	magnetite
#8	AM33-2-2a	0.01	31.83	0.00	0.01	27.15	8.96	0.00	0.16	0.00	31.74	99.87	ilmenite

Table 4: AAS analysis (in ppm except MnO and Fe₂O₃) of rock samples from Tira underground mine, Buteba granite and along River Solo

SAMPLE	TYPE	Location	Au	Cu	Ni	Co	Zn	Pb	MnO%	Fe ₂ O ₃ %
AM 4	Basalt	River Solo	-	54	50	65	300	20	0.114	8.571
AM 16	Basalt	28-subdrive	-	83	30	41	200	30	0.692	16
AM 17	Basalt	28-subdrive	-	38	20	38	320	20	0.485	10.571
AM 23	Basalt	45N-drive	-	1640	330	105	1840	120	0.294	8
AM 24	Quartz vein	45N-drive	4.8	183	20	127	4920	180	0.046	0.571
AM 33	Basalt	28S/N-drive	0.1	103	80	55	560	30	0.687	19.143
AM 34	Basalt/Quartz vein	28S/N-drive	2.1	92	10	87	220	120	0.235	5.143
AM 36	Basalt	28-subdrive	0.7	290	40	45	440	40	0.349	9.714
AM 38	Basalt	28-subdrive	-	198	100	53	200	70	0.367	8.286
AM 40	Basalt/Quartz vein	28-subdrive	6.8	80	40	58	200	460	0.183	7.143
AM 81	Granite	Buteba	-	3	10	45	180	40	0.026	0.857
AM 83	Granite	Buteba	-	3	10	77	100	40	0.031	1.429

Table 5: Variation of metal content with depth of the soil samples from the Tira open pit mine (Analysis is by AAS and values are in ppm, except MnO)

SAMPLE	DEPTH (m)*	Au	Ag	Cu	Ni	Zn	Pb	MnO%
AM 63	14	4	1	153	40	309	190	0.019
AM 66	12.5	0.8	1	43	40	131	40	0.039
AM 69	11	6.2	1	44	40	157	30	0.003
AM 72	9.5	6.8	1.5	108	90	330	620	0.17
AM 75	8	7.4	1.5	92	60	332	110	0.011

Table 6: Results of AAS analysis of soil and stream sediment samples from the study area (Trace element values in ppm, MnO in %)

SAMPLE	TYPE	Au	Ag	Cu	Ni	Zn	Pb	MnO%
AM5	Rv*	0.2	0.5	52	70	67	30	0.003
AM9	Rv	2	2	119	110	72	90	0.338
AM14	Rv	0.2	0.5	40	50	63	30	0.003
AM63	Sl-pit*	4	1	153	40	309	190	0.019
AM66	Sl-pit	0.8	1	43	40	131	40	0.039
AM69	Sl-pit	6.2	1	44	40	157	30	0.003
AM72	Sl-pit	6.8	1.5	108	90	330	620	0.17
AM75	Sl-pit	7.4	1.5	92	60	332	110	0.011
AM84	Rv	38.6	3	366	60	234	1250	0.279
AM86	Rv	16.4	10.5	262	40	155	720	0.072
AM87	Rv	30.4	2.5	204	60	356	990	0.351
AM89	Rv	20.2	9	243	70	253	2510	0.251
AM90	Rv	19.4	2.5	106	80	87	250	0.157
AM91	Rv	1.8	1	93	100	68	60	0.006
AM92	Rv	3.6	0.5	78	90	52	40	0.085
AM93	Rv	4.4	0.5	95	100	80	50	0.392
AM99	Rv	0.2	1	126	100	72	130	0.013
AM101	Sl*	2.8	0.5	58	60	77	30	0.003
AM103	Sl	0.8	0.5	122	100	118	40	0.004
AM106	Sl	0.6	1	72	50	108	40	0.004
AM110	Sl	1.8	1	92	100	123	30	0.003
AM111	Rv	0.4	1	92	90	86	50	0.005
AM118	Rv	0.2	0.5	39	60	45	40	0.004
AM121	Rv	0.2	0.5	36	50	50	30	0.003
AM122	Rv	0.2	0.5	16	30	37	30	0.003
AM123	Sl	0.6	0.5	105	110	92	50	0.238
AM124	Sl	0.8	1	79	100	85	40	0.004
AM126	Sl	0.4	0.5	85	70	89	40	0
AM129	Sl	0.8	0.5	107	120	76	20	0.15
AM130	Sl	0.6	1	113	110	93	50	0.005
AM131	Sl	0.4	1	96	120	96	30	0.108
AM132	Sl	0.2	1	79	100	89	40	0.004
AM133	Sl	0.4	1	58	90	67	30	0.046
AM134	Sl	0.6	1	73	90	87	30	0.003
AM135	Sl	1.6	0.5	31	60	40	30	0.044
AM139	Sl	0.4	1	89	100	96	30	0.145
AM141	Rv	0.6	1	95	80	69	60	0.006
AM144	Rv	0.4	1	47	50	49	40	0.004
AM166	Sl	0.2	0.5	86	100	100	30	0.003
AM168	Sl	0.6	1	72	80	83	30	0.003
AM171	Sl	0.4	1	96	90	83	30	0.003
AM177	Sl	0.4	1	84	120	77	30	0.003
AM181	Sl	0.2	1	73	90	69	30	0.003
AM185	Sl	0	1	71	80	87	10	0.001
AM187	Sl	4.8	-	111	110	73	30	0.183

* Rv – Stream sediment; Sl – Soil sample; Sl-pit – Soil sample from Tira mine open pit

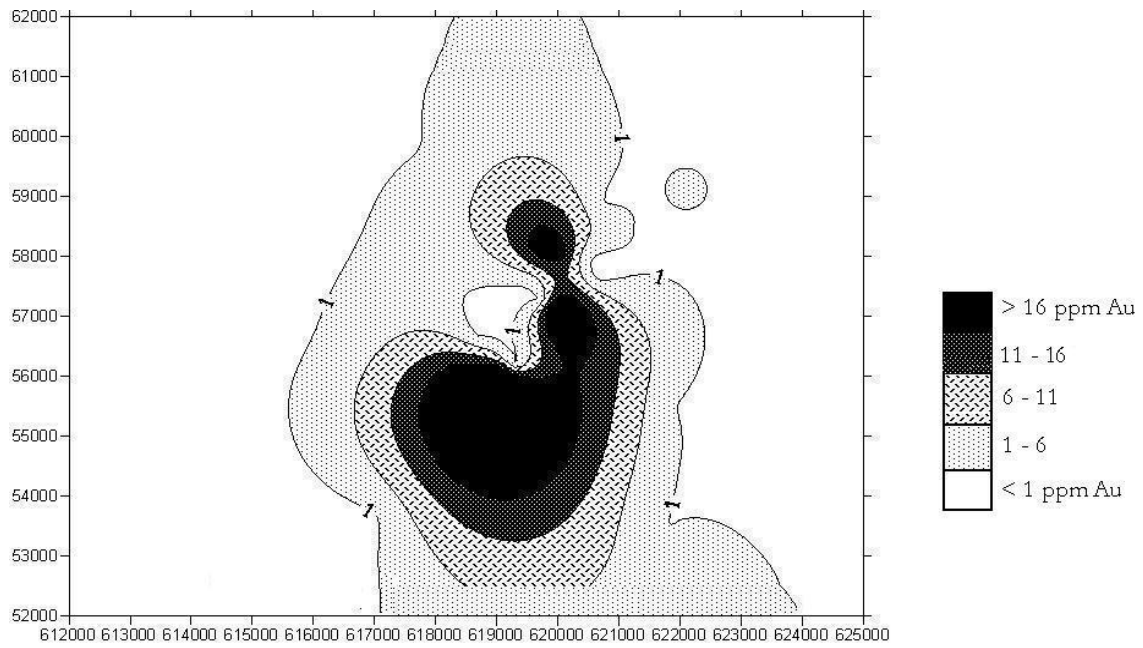


Figure 13: The gold anomalies of both soil and stream sediment samples

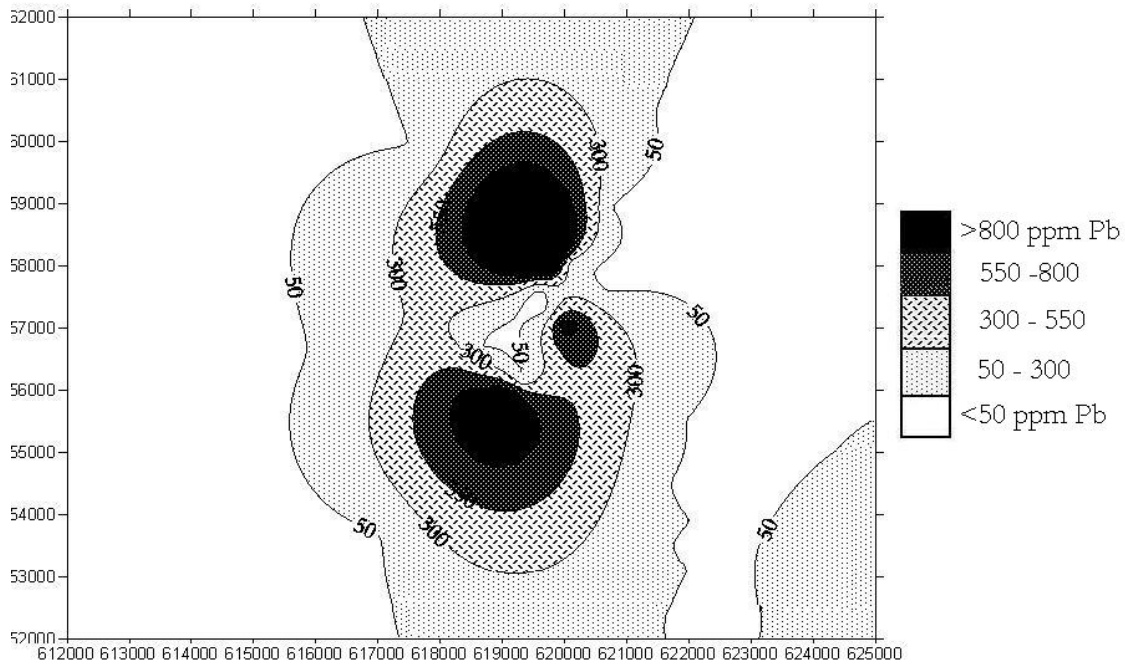


Figure 14: The lead anomalies of both soil and stream sediment samples

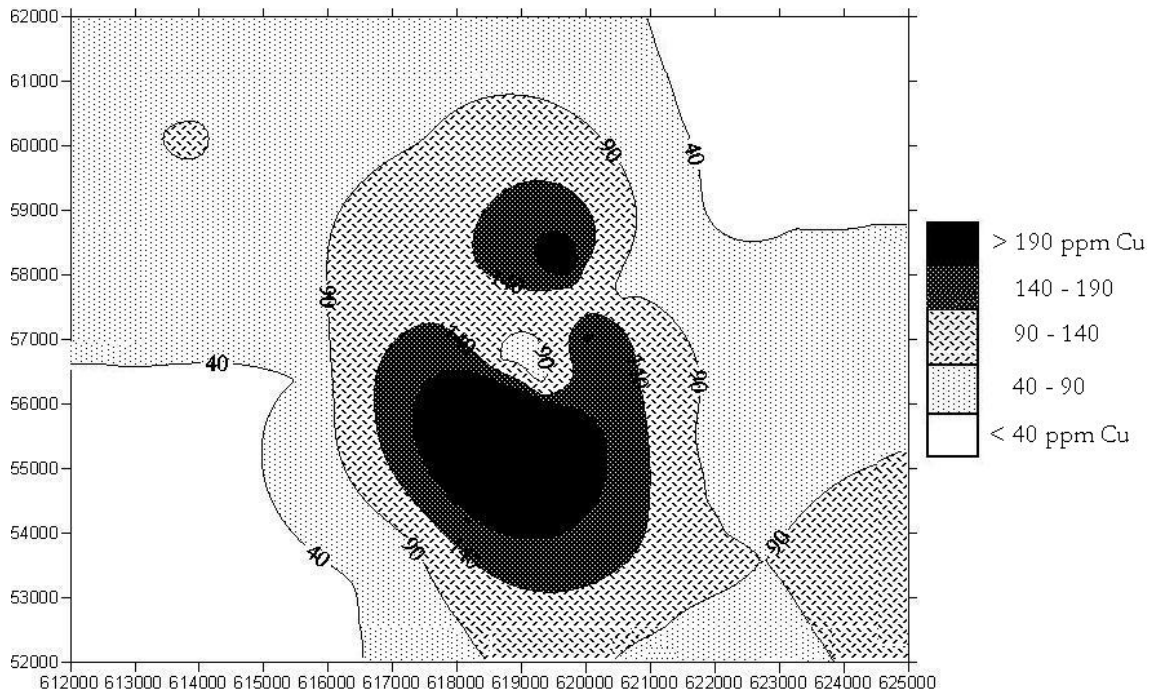


Figure 15: The copper anomalies of both soil and stream sediment samples

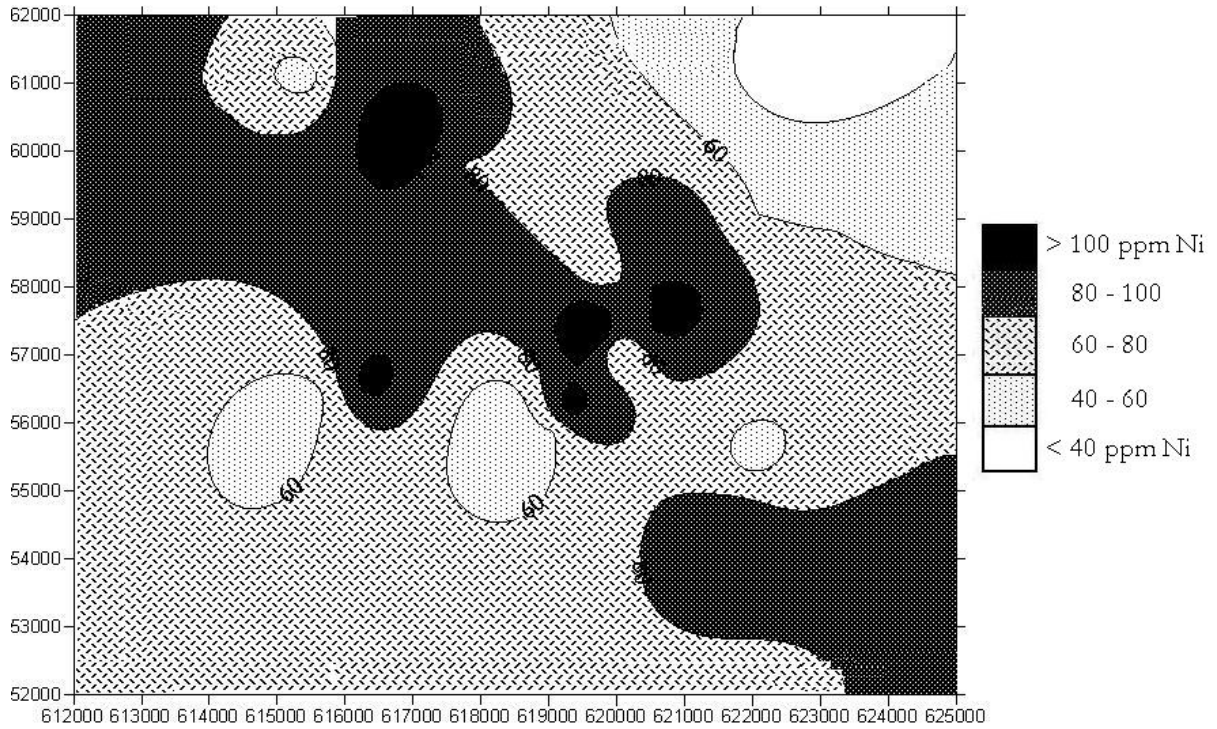


Figure 16: The nickel anomalies of both soil and stream sediment samples

DISCUSSION

The rock samples selected for study were those rich in visible sulphides and this was not the case with the BIF hosted deposits in which mineralisation is mostly disseminated. EMP analysis was therefore done for the quartz vein hosted deposits only. These were formed by mineralising fluids that intruded the basaltic country rock through already existing NW-trending fractures (probably related to the Pan African event and the Aswa shear zone). The fluids brought about a mineral assemblage of pyrite and other sulphides like pyrrhotite, chalcopyrite, galena, covellite and oxides like magnetite and ilmenite which are to be found in both the quartz veins and the surrounding basaltic rocks. The fluids also altered the country rock leading to the formation of secondary minerals like chlorite, sericite, epidote, zoisite, calcite, sphene and goethite.

Gold occurs as electrum and native gold inclusions in pyrite. The inclusions are a solid solution of gold and silver with trace amounts of Bi, Cu and Pb. The element maps of some electrum grains for Au, Ag and Bi and BSE photomicrographs (Figs. 10–13) show that these elements are homogeneously distributed which implies their co-precipitation. Even bismuth which is of trace amounts is evenly distributed throughout the grains (Fig. 12). Fineness of gold is between 451–863. Of the 16 inclusions analysed, six are classified as native gold and the rest as electrum (Table 1).

In addition a significant amount of gold occurs as invisible gold in pyrite and other sulphides. However the other sulphides are not important hosts of gold given their insignificant volume %. The values of invisible gold in pyrite are in the range of 0–0.57 wt% (an average of 0.18 wt% or 1800 ppm). According to Michel et al. (1994), the gold values of the As-rich pyrite of the Santa Rita gold vein deposits in Brazil, which is an entirely invisible gold deposit, are up to 100 ppm Au. Pals et al. (2003) carried out microprobe analyses (EMP and SIMS) on samples from the Emperor gold deposit of Fiji and noted that the values of gold (the highest being 11,057 ppm) in the pyrite of these deposits were among the highest yet reported. Using an average value of 507 ppm Au for the pyrite grains analysed and assuming the proportion of pyrite in the ore by volume to be between 0.5–1.0%, they estimated the amount of invisible gold in these deposits to be 47–92% of total gold. The volume % of pyrite in the Busia ore is probably in the same range as that in the Emperor deposits, in which case invisible gold may be equally important in this deposit. Invisible gold is usually inaccessible to traditional extraction methods and if not recognised at an early stage could lead to loss of gold into the tailings

(Ashley et al., 2000, Larocque et al., 2002). It is therefore important to establish how much in these deposits is invisible gold so that any losses that may be taking place currently are stopped.

Apart from pyrite, the only other minerals with significant volume % are magnetite and ilmenite. Larocque et al. (2002) noted that these minerals are of equal importance to pyrrhotite and chalcopyrite as hosts for gold in magmatic systems and that in sulphide deficient rocks and oxidised felsic intrusions, they were the most important. The gold in them is usually invisible and inaccessible to traditional recovery techniques and so needs to be quantified in order to determine the extraction method to be used. The EMP analyses of the Busia deposits however show that there is no detectable gold in both magnetite and ilmenite. The values of manganese in ilmenite (Table 3) are as high as 8.96 wt % which implies that the solution from which ilmenite was formed was manganese-rich. Manganese replaces iron in ilmenite and to a lesser extent in magnetite. The gold values of stream sediments average 7.7 ppm Au, the highest being 38.6 ppm Au (Table 5). This is unlike the soil samples which are all less than 4.8 ppm Au with the exception of some from the open pit mine at Tira. This shows that streams play an important role of concentration of the mineralisation. They also however lead to dispersion and ‘dilution’ of the gold. This may explain why the gold values are high upstream (e.g. River Nakola) and lower downstream. The major gold soil anomalies observed are in the Tira area, north and south of the present workings. Of the other areas proposed by Mroz et al. (1991) for follow-up, Osapiri which has the highest value as 2.8 ppm Au is next in ranking. The highest value in the Bukade-Makina area is 0.6 ppm Au. The gold mineralisation in Osapiri and Bukade-Makina areas probably originates from the BIF in the area in which the mineralisation is perhaps disseminated while that from Tira area is from the quartz vein deposits.

The anomalies of Pb, Cu, Zn and Ag coincide with those of gold (Figs. 14–18) while there is completely no similarity with nickel (Fig. 19). This may mean that the source of the nickel mineralisation is different from that of Au, Cu, Pb, Zn and Ag. It is most probable that the nickel is from the mafic country rocks (the metabasalts of the greenstone belt) while these other elements are from the sulphides introduced by epigenetic solutions which formed the quartz veins. Therefore, Pb, Cu, Ag and Zn can be used as indicator (pathfinder) elements for gold. In addition, lead has a high positive correlation (+0.9) with gold in the rocks (Table 4). This marks it out as the most reliable indicator element for gold in the Busia deposits.

From the samples taken from the wall faces of the Tira open pit mine, the concentration of gold generally decreases with increasing depth (Table 6). This may indicate that the mineralisation is not related to the underlying rocks but to the epigenetic solutions. The last solutions crystallising to form veins (which is at the uppermost level reached by the veins) were gold richer. Moreover the veins pinch upwards. This was probably a result of the decreasing amount of fluids but may in turn have led to a concentration of gold. The gold could also have been transported as hydrosulphide complexes ($\text{Au}(\text{HS})_2$) along fractures with reduction in pressure and temperature resulting in breakdown of the complexes and gold deposition (Tolessa, 1999). In addition, given that calcite forms as a secondary mineral the gold could also have been carried as CO_3 complexes.

CONCLUSION

There are two types of gold mineralisation in the Busia area; the quartz vein-hosted deposits and the BIF-hosted deposits. In the present study, the bulk of the EMP analyses are of the quartz vein deposit type of the Tira area and these indicate great economic potential. The soil and stream sediment sampling around the BIF in the Osapiri and Bukade-Makina areas also suggests possibility of economic potential. Further work is therefore necessary to ascertain their actual characteristics and potential.

The ore minerals in the quartz vein deposit at Tira include gold, pyrite, pyrrhotite, chalcopyrite, galena, covellite, magnetite and ilmenite. The host rocks which are basaltic rocks are rich in secondary calcite. Gold occurs as native gold or electrum inclusions in pyrite with fineness of 451 – 863. It also occurs as invisible gold in pyrite, pyrrhotite, chalcopyrite and galena. The EMP analyses of the sulphides and their comparison with other deposits worldwide in which invisible gold is important, show that invisible gold in pyrite may contribute significantly to the gold budget of the Busia deposits.

Soil gold anomalies were found in the areas of Tira (4.8 ppm Au) and Osapiri (2.8 ppm Au). The highest value in the Bukade-Makina area was 0.6 ppm Au and so this area is not as interesting as the other two. The soil anomaly in the Tira area is probably coming from the quartz vein deposit while the source of the mineralisation in the other two areas is probably the BIF, in which the gold mineralisation is perhaps disseminated. Stream sediment anomalies were found on Rivers Nakola, Tira and Aget, the highest being, 38.6 ppm Au. The source of

mineralisation in this area is the quartz vein deposit at Tira.

Lead (Pb) has very high positive correlations with gold in all types of samples and so is the most reliable indicator element for gold. Copper, silver and zinc may also be used as indicator elements for gold in the Busia deposits.

In the present study, geochemical analysis of the BIF at Bukade-Makina and Osapiri was not done. This is necessary in order to know their extent and economic importance. More work (e.g. isotope, REE and Age determination studies) also needs to be done to determine the genesis of both deposit types in the area. It is also necessary to find out the viability of the old workings in the Amonikakinei sector and of the surrounding areas.

Future systematic sampling and analysis of pyrite, which is the only sulphide with a significant volume proportion, is necessary to confirm the contribution of the invisible gold to total gold. In addition, it is necessary to know if all or only some pyrite in the quartz veins and the metabasalts contains gold.

ACKNOWLEDGEMENTS

We wish to express our gratitude to Prof. Dr. M. Tarkian and the staff of the Institute of Mineralogy and Petrology of the University of Hamburg for their invaluable help during the Electron Microprobe analysis and to the German Academic Exchange Service (DAAD) who sponsored this research work. We are also grateful to Busitema Mining Co. Ltd. for granting us unlimited permission to work on their property and for all the assistance they offered us. We are also indebted to the laboratory staff of the Geology Department at Makerere University for their tremendous assistance.

REFERENCES

- Ashley, P. M., Creagh, C. J. and Ryan C. G. 2000. Invisible gold in ore and mineral concentrates from the Hillgrove gold-antimony deposits, NSW, Australia. *Journal Mineralium Deposita* **35**, 285-301.
- Closs, L. G. 1997. Exploration geochemistry: Expanding contributions to the mineral resource development. In: *Keynote Session Proceedings of Exploration 97: Fourth Decennial International Conference on Mineral Exploration*. (Edited by Gubins, A. G) pp 3 – 8. Toronto, Canada.
- Hester, B. and Boberg, W. 1996. *Uganda, Opportunities for mining investment*. 56p. Brian W. Hester Inc., Denver, Colorado, USA.

- Larocque, A.C.L., Stimac, J.A., McMahon, G., Jackman, J.A., Chartrand, V.P., Hickmott, D. and Gauerke, E. 2002. Ion-Microprobe analysis of *FeTi* oxides: Optimisation for the determination of invisible gold. *Bulletin Society Economic Geologists* **97**, 159-164.
- Michel, D., Giuliani, G., Olivo, G. R. and Marini, O. J. 1994. As growth banding and the presence of Au in pyrites from the Santa Rita gold vein deposit hosted in Proterozoic metasediments, Goiás State, Brazil. *Bulletin Society Economic Geologists* **89**, 193-200.
- Mroz, J. P., Urien, P., Baguma, Z. and Viallefond, L. 1991. Gold exploration in Busia area, Uganda (Phase 1). *Report R 32761*, 120p. Bureau de recherches géologues et minières (BRGM).
- Old, R. A. 1968. The geology of part of south east Uganda. Ph. D. dissertation 138p. Research Institute of African Geology, Department. of Earth Sciences, University of Leeds.
- Pals, D. W., Spry, P. G. and Chryssoulis, S. 2003. Invisible gold and tellurium in arsenic-rich pyrite from the Emperor gold deposit, Fiji: Implications for gold distribution and deposition. *Bulletin Society Economic Geologists* **98**, 479-493.
- Rwabwoogo, M. O. 1998. Uganda districts information handbook. 152p. Fountain Publishers, Ltd, Kampala. 5th Edition.
- Tolessa, D. 1999. The geology, geochemistry and genesis of Legadambi and Moyale gold deposits. Ph. D. dissertation 165p. Institut für Geowissenschaften Technische Universität, Braunschweig.
- Xie, X. and Wang, X. 1991. Geochemical exploration for gold: a new approach to an old problem. *Journal Geochemical Exploration* **40**, 25-48.